INORGANIC CHEMISTRY FRONTIERS

RESEARCH ARTICLE

View Article Online
View Journal | View Issue

Cite this: *Inorg. Chem. Front.*, 2023, **10**, 6401

Manipulating pre-equilibria in olefin polymerization catalysis: backbone-stiffening converts a living into a highly active salan-type catalyst†

Dmitry V. Uborsky, *[a] Mikhail I. Sharikov,[a] Georgy P. Goryunov, [a] Kristina M. Li,[a] Anna Dall'Anese,[b,d] Cristiano Zuccaccia,*[b,d] Antonio Vittoria, [c,d] Teresa Iovine,[c] Gianluigi Galasso,[c] Christian Ehm, [c,d] Alceo Macchioni, [b,d] Vincenzo Busico, [c,d] Alexander Z. Voskoboynikov [a] and Roberta Cipullo *[c,d]

Received 4th August 2023,
Accepted 21st September 2023

DOI: 10.1039/d3qi01537h

rsc.li/frontiers-inorganic

Stiffening of the catalyst backbone of salan-type catalyst **1** *via* ring closure yields indanosalan **3** and increases activity and molar mass capability by two orders of magnitude. In propene polymerization, catalyst **3** is highly isotactic selective and nearly as active as one of the most productive known salan-catalysts today (**2**), showing much higher molar mass capability. NMR studies provide evidence of the identity of the active metal-polymeryl species for the catalyst pair **1**/**3**, explaining their vast activity differences: the traditional salan catalyst **1** is trapped in the inactive *mer–mer* configuration, while indanosalan **3** prefers the active *fac–fac* isomer.

Introduction

Pre-equilibria in catalysis can "make[1–3] or break[4–7]" a catalyst. In the specific case of olefin polymerization, *e.g.*, formation of mixed-metallic species between the active catalyst and other components of the catalytic pool can slow the catalyst down.[4,8–13] Another prominent example is the formation of more stable but catalytically inactive isomers.[5,6,14] Post-metallocene catalysts of the bis(phenoxy-amine) family ("salan-type"), first introduced by Kol,[15–18] offer a striking example in this respect. The inherent flexibility of the tetradentate [ONNO] ligand (L) allows it to wrap around the metal in various ways,[14] leading to multiple energetically accessible isomers (*fac–fac*, *fac–mer*, *mer–mer*, named after the *fac* or *mer* geometries of the two [ONN] fragments, see Fig. 1).

The C_2-symmetric *fac–fac* isomer is generally favored in neutral precatalysts LMR_2 of group 4 metals (R = Bn, Me_2CHO).[15,19] Contrarily, the *mer–mer* isomer is often the most stable isomer for pentacoordinated active cations adopting a distorted square pyramidal geometry as demonstrated by solution NMR spectroscopy and DFT.[5,6,20]

Since after activation the coordination vacancy is *trans* to the R group in the cationic *mer–mer* isomer, these species are polymerization inactive. For catalysts preferring the *mer–mer* isomer, isomerization to the *fac–fac* isomer is required prior to

[a]*Department of Chemistry, Lomonosov Moscow State University, 119991 Moscow, Russia. E-mail: duborsky@med.chem.msu.ru*
[b]*Dipartimento di Chimica, Biologia e Biotecnologie, Università degli Studi di Perugia and CIRCC, 06123 Perugia, Italy. E-mail: cristiano.zuccaccia@unipg.it*
[c]*Dipartimento di Scienze Chimiche, Università di Napoli Federico II, 80126 Napoli, Italy. E-mail: rcipullo@unina.it*
[d]*DPI, 5600 AX Eindhoven, The Netherlands*

†Electronic supplementary information (ESI) available: Synthetic procedures and characterization, detailed NMR spectra, polymerization procedures, polymer characterization procedures, and polymer analytical characterizations, computational details for conformer sampling (PDF). Coordinates for DFT structures (*XYZ*). CCDC 2283479. For ESI and crystallographic data in CIF or other electronic format see DOI: https://doi.org/10.1039/d3qi01537h

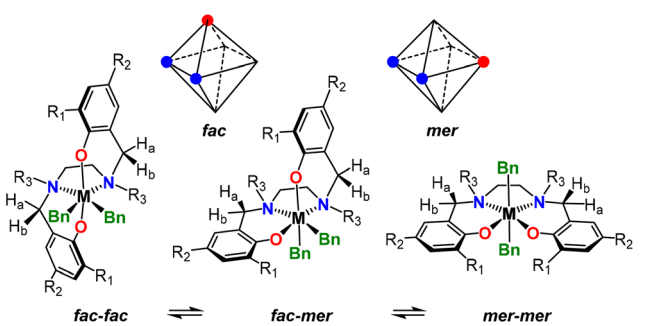

Fig. 1 Illustration of the *fac* and *mer* isomerism for octahedral compounds (top) and of the possible isomers for salan precatalyst (bottom).

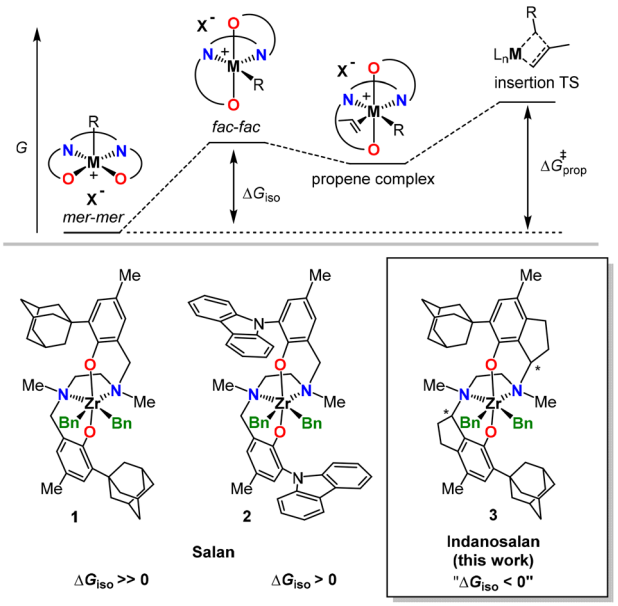

Fig. 2 Top: Idealized energetic profile of propene insertion, starting from the *mer–mer* isomer (ΔG_{iso} = free energy difference between *fac–fac* and *mer–mer* isomers; $\Delta G^{\ddagger}_{prop}$ = propagation barrier). Bottom: salan complexes **1** (slow catalyst) and **2** (fast catalyst) with flexible catalyst backbone and novel indanosalan **3** with a rigid skeleton.

olefin insertion ($\Delta G_{iso} > 0$) and passes through the *fac–mer* isomer.[5,6] This pre-equilibrium is integral part of the propagation barrier (Fig. 2) and responsible for the often at best sluggish activity of salan catalysts with α-olefins.[15,19]

Phenolate ring substituents (Fig. 1) strongly influence catalyst performance in propene polymerization: (a) both R_1 and R_2 can affect activity and regioselectivity through electronic effects,[19] (b) R_1 influences stereo- and regioselectivity *via* steric effects,[15,19] and (c) R_1 substituents can also alter the *fac–fac*/*mer–mer* equilibrium *via* sterics.[6] The non-obvious coupling of the latter two effects complicates rational tuning. On the other hand, we have recently shown that limiting catalyst flexibility can dramatically increase catalyst performance,[21] even in systems as well studied as *ansa*-metallocenes.[22,23]

Employing a conceptually similar approach, we reasoned that locking salan-type catalysts in the polymerization active *fac–fac* isomer through stiffening of the catalyst backbone should improve their activity. In particular, the interconversion of the *mer–mer* into the *fac–fac* isomer or *vice versa* requires a rotation around the carbon–carbon bond between the methylene spacer and the phenyl ring (Fig. 1 and ESI†), which can be "easily" blocked *via* ring-closure.

As proof of principle, we designed and synthesized a novel indanosalan catalyst bearing an *ortho*-1-adamantyl substituent in position R_1 (**3**, Fig. 2). We chose the *ortho*-1-adamantyl substituted salan,[19] because catalyst **1** in Fig. 2 is highly isotactic selective in propene polymerization showing low activity, to the point that was used to synthesize well-defined iPP-*block*-PE copolymers.[24]

Results and discussion

Indanosalan **3** has four stereocenters (two chiral N and two chiral C atoms). DFT calculations indicate that for a given *rac*-isomer with respect to the two chiral carbon atoms, *mer–mer* and *fac–fac* isomers of **3** differ in the chirality of the N-bridge atoms; direct isomerization with retention of chirality at N is impossible, as ring closure blocks rotations and we could not locate such an isomer employing Grimme's conformer–rotamer ensemble sampling tool (CREST)[25] followed by subsequent full DFT optimization of identified conformers at the TPSSh-D_{zero}(PCM)/TZ//TPSSh/DZ level of theory.[26–31] Instead, isomerization requires N-decoordination and umbrella inversion at both nitrogen atoms. As a consequence, **3** should be kinetically trapped in the *fac–fac* isomer, at least on the timescale of a typical polymerization.

The key step in the assembly of the indanosalan ligand **3d** (Scheme 1) was alkylation of *N*,*N*′-dimethylethylenediamine with indanol **3c**. Due to the presence of two stereocenters in **3d** a mixture of *rac*- and *meso*-isomers of the ligand was expected. Surprisingly, a single compound precipitated from the reaction mixture in 72% yield. ^{1}H and ^{13}C NMR spectra agreed with the structure of the ligand but did not allow positive identification of the diastereomer. Reaction of the isolated ligand with $ZrBn_4$ cleanly afforded a single, C_1-symmetric, $ZrBn_2$ complex. Activation with $Ph_3C^+B(C_6F_5)_4^-$/tri-*iso*-butyl aluminum (TTB/TiBA) in the presence of 1-hexene yielded no polymer, strongly indicating that the isolated ligand was *meso*-**3d**.

Selective formation of one diastereomer points to a reversible mechanism[33] involving an *o*-quinone methide intermediate.[34] Consequently, under the reaction conditions, the two diastereomers of the ligand should be in equilibrium, which is shifted by precipitation of *meso*-**3d**. Taking advantage of this reversibility, a ~1 : 1 *rac*/*meso*-**3d** mixture was prepared from pure *meso*-**3d** through stirring a hot dilute solution of *meso*-**3d** in toluene overnight followed by quick cooling to room temperature to "freeze" the equilibrium. Subsequently, selective precipitation of *meso*-**3d** yielded a solution of *rac*-**3d** pure enough for metalation. Reaction of *rac*-**3d** with $ZrBn_4$ in toluene yielded a mixture of C_2- (*fac–fac*, *rac*-$\mathbf{3}_{FF}$) and C_1- (presumably

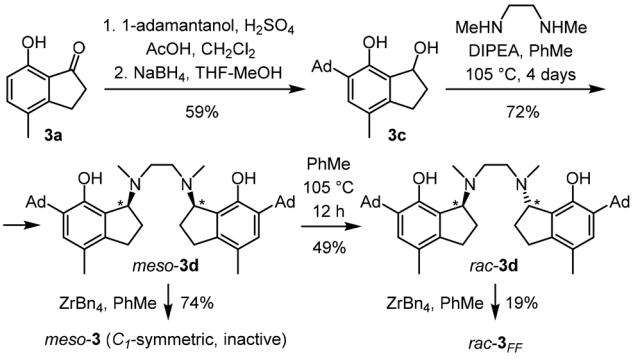

Scheme 1 Synthesis of *meso*-**3** and *rac*-$\mathbf{3}_{FF}$ from **3a**.[32]

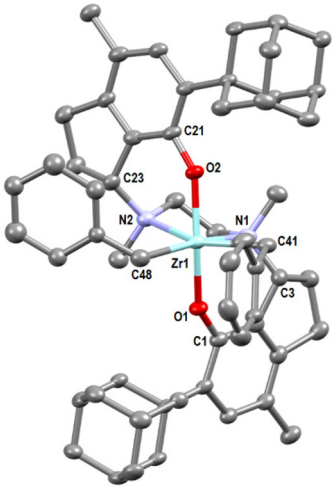

Fig. 3 X-ray crystal structure of *rac*-$\mathbf{3}_{FF}$. Hydrogen atoms omitted for clarity; ellipsoids drawn at 50% probability level. The left Zr-benzyl moiety is disordered, one of the two local minima is shown. Selected bond lengths (Å): Zr1–C41 2.285(4), Zr1–C48 2.306(4), Zr1–O1 2.000(2), Zr1–O2 2.002(2), Zr1–N1 2.552(3), Zr1–N2 2.485(3). Selected angles (°): C41–Zr1–C48 106.20(14), N1–Zr1–N1 72.06(10), C1–O1–Zr1 146.2(2), C21–O2–Zr1 145.4(2).

fac–mer, *rac*-$\mathbf{3}_{FM}$) isomeric complexes in 61% yield from which *rac*-$\mathbf{3}_{FF}$ was isolated through crystallization in 19% yield. Unlike *meso*-**3**, *rac*-$\mathbf{3}_{FF}$ polymerizes 1-hexene when activated with TTB/TiBA.

The X-ray crystal structure of *rac*-$\mathbf{3}_{FF}$ is shown in Fig. 3. The complex adopts a slightly distorted C_2-symmetric octahedral geometry. The additional ring closures introduce obvious changes in the bond angles and torsions around the two spacer carbons C3 and C23; nonetheless, those changes do not translate into significantly different parameters of the coordinational polyhedron in comparison with those in adamantyl-substituted salan complexes known in the literature,[35,36] as the O–N distances remain nearly the same.

Low-temperature NMR studies provide insight into the reaction of 1-hexene with **1-Bn**$^+$ and **3-Bn**$^+$, generated in C_6D_5Cl by adding one equivalent of TTB to **1** and **3**.

At 233 K, **1-Bn**$^+$ is predominantly present in the form of the *fac–fac* isomer, as indicated by the characteristic ^{13}C NMR chemical shift of the NMe groups (>40 ppm for both, Fig. 4a).[37] Addition of ~15 equiv. of 1-hexene resulted in the slow consumption of both 1-hexene and **1-Bn**$^+$ along with the formation of a new, relatively stable, organometallic species. Given the known living nature of this catalyst, we formulate it as **1-P$_n$**$^+$. The majority of **1-P$_n$**$^+$ accumulates in the form of the inactive *mer–mer* isomer as evidenced by ^{13}C NMR chemical shifts of the NMe groups at 37.6 and 42.6 ppm (Fig. 4b).[37]

The possibility to prepare the *rac*-**3** metal complex as a mixture of both *fac–fac* and *fac–mer* isomers offered the unique opportunity to study their chemical equilibria. Upon activation of a 3 : 2 mixture of *rac*-$\mathbf{3}_{FM}$/*rac*-$\mathbf{3}_{FF}$, the ^{13}C NMR spectrum shows a 2 : 1 mixture of the *fac–fac* and *fac–mer* isomers of

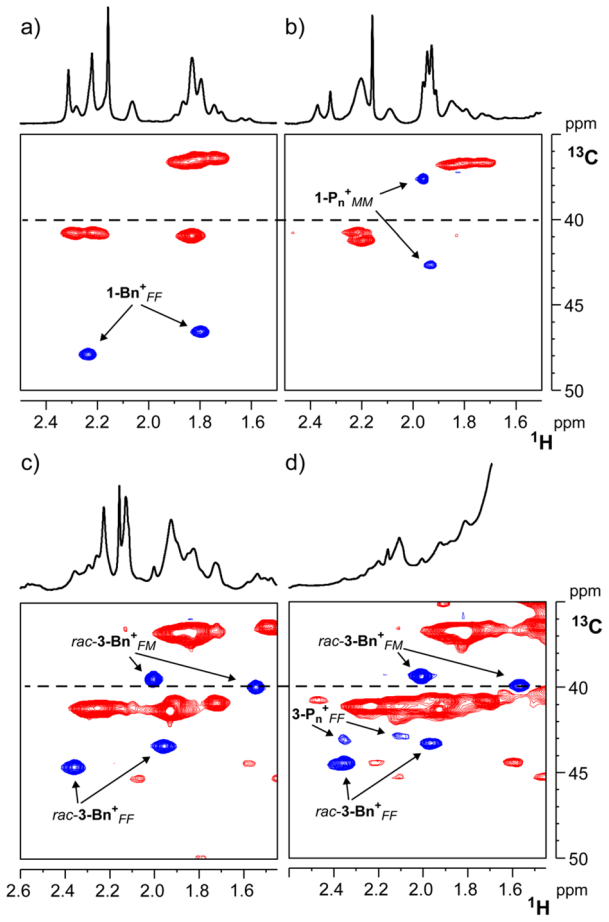

Fig. 4 Sections of four multiplicity-edited ^{1}H,^{13}C HSQC NMR experiments (blue cross peaks = CH or CH_3 moieties) relative to the NMe region and showing: (a) the *fac–fac* isomer of **1-Bn**$^+$; (b) formation of the *mer–mer* isomer of **1-P$_n$**$^+$ after the addition of 15 equiv. of 1-hexene to **1-Bn**$^+$; (c) the mixture of *fac–fac* and *fac–mer* isomers of **3-Bn**$^+$ derived from a 3 : 2 mixture of *rac*-$\mathbf{3}_{FM}$/*rac*-$\mathbf{3}_{FF}$; (d) formation of the *fac–fac* isomer of **3-P$_n$**$^+$ after the addition of 460 equiv. of 1-hexene to **3-Bn**$^+$. All experiments were carried out in C_6D_5Cl at 233 K.

3-Bn$^+$ (δ_C = 43.4 and 44.6 ppm for the *fac–fac*, 39.5 and 39.9 ppm for the *fac–mer*, respectively; Fig. 4c). Chemical exchange between *fac–fac* and *fac–mer* isomers of **3-Bn**$^+$ is slow on the NMR time scale, indicating substantial barriers for isomerization as pointed out by DFT calculations (*vide supra*). The rate of site epimerization at the *fac–fac* isomer is not dissimilar to that of **1-Bn**$^+$ under similar conditions: k_{SE} = 0.6 s^{-1} at 223 K and 0.4 s^{-1} at 228 K, for $\mathbf{3}_{FF}$-**Bn**$^+$ and **1-Bn**$^+$, respectively. Addition of ~15 equiv. of 1-hexene to the mixture leads to immediate formation of poly-1-hexene, without apparent consumption of either **3-Bn**$^+$ species. However, addition of a larger excess of 1-hexene (~460 equiv.) resulted in a substantial consumption of $\mathbf{3}_{FF}$-**Bn**$^+$ but not $\mathbf{3}_{FM}$-**Bn**$^+$, indicating the latter is inactive (or much less active). In turn, $\mathbf{3}_{FF}$-**Bn**$^+$ displays the typical behavior of a very active olefin polymerization catalyst, *i.e.*, the first olefin insertion is much slower than subsequent insertions.[38]

A prolonged ^{1}H,^{13}C HSQC NMR experiment (Fig. 4d), lasting several hours from the addition of 1-hexene, allowed

Table 1 Propene polymerization results (averaged on at least triplicate experiments) using **1**, **2** and **rac-3**$_{FF}$ at T_p 60 °C and $p_{propene}$ = 6.6 bar

Precatalyst	R_p [a]	σ [b]	[2,1] %	M_n, kDa	M_w, kDa	PDI
1	0.19	0.998	0.52	7.6	14	1.8
2	17	0.82	0.80	1.3	2.0	1.5
rac-**3**$_{FF}$	38	0.994	0.53	113	248	2.2

[a] In kg_{PP} $mmol_{Zr}^{-1}$ h^{-1}. [b] Probability to select the preferred monomer enantioface at an active site of given chirality.

detection of two new ^{13}C NMR resonances in the region of the NMe groups, tentatively assigned to a **3-P$_n^+$**$_{FF}$ species. While complete identification of this species is hampered by the poly-1-hexene signals, the NMe chemical shifts (δ_C > 40 ppm) clearly indicate that the active species, differently from **1-P$_n^+$**, retains *fac–fac* geometry.

The novel indanosalan catalyst *rac*-**3**$_{FF}$, the parent salan **1** and the *ortho-N*-carbazolyl salan **2**, which is one of the most active salan [ONNO]Zr propene polymerization catalysts presently known and mildly isotactic selective,[6,39] have been tested in propene polymerization at 60 °C using MAO/BHT[8,40–44] as activator (Table 1) in a high-throughput experimentation platform (Freeslate parallel pressure reactor, PPR).[45–49] The polymerization procedure is reported in the ESI† and described in more detail in ref. 22, 23 and 50.

Inspection of Table 1 reveals that the ligand modification, leading to the novel precatalyst *rac*-**3**$_{FF}$, yields a dramatic enhancement of catalyst productivity (R_p), exceeding its homologue (**1**) by over two orders of magnitude and even surpassing the performance of **2**. Strikingly, the catalyst derived from *rac*-**3**$_{FF}$ also shows a much higher polymer molar mass capability compared with both **1** and **2** (Table 1). This indicates that the **3-P$_n^+$**$_{FF}$ active species (P_n = growing polymeryl) features a higher ratio between the apparent rates of chain propagation and chain transfer than both **1-P$_n^+$** and **2-P$_n^+$**. Neither stereo- nor regioselectivity are affected by the ligand modification and no indications for the loss of C_2-symmetry under polymerization conditions are observed, indicating that the catalyst is stable under polymerization conditions.

Conclusions

rac-**3**$_{FF}$ precatalyst has been designed and synthetized *ad hoc* to hamper, during propene polymerization, the *fac–fac*/*mer–mer* isomerization, responsible for the poor activity of most salan-type catalysts. Gratifyingly, *rac*-**3**$_{FF}$, upon activation with MAO/BHT, polymerizes propene with a productivity that exceeds one of the most active salan-type catalysts (**2**) and with almost two orders of magnitude higher molecular mass capability.

Data availability

Crystallographic data has been deposited at the CCDC with number 2283479.† Synthetic procedures and characterization, detailed NMR spectra, polymerization procedures, polymer characterization procedures, and polymer analytical characterizations, computational details for conformer sampling are reported in the ESI.†

Author contributions

The manuscript was written through contributions of all authors. All authors have given approval to the final version of the manuscript.

Conflicts of interest

There are no conflicts to declare.

Acknowledgements

The work of ADA, CZ, AV, CE, RC, AM and VB forms part of the research programme of DPI, project #835. The authors wish to express their gratitude to P. H. M. Budzelaar for helpful discussions. AM and CZ also thank the European Union – NextGenerationEU under the Italian Ministry of University and Research (MUR) National Innovation Ecosystem grant ECS00000041 – VITALITY for supporting this work. AM and CZ also acknowledge Università degli Studi di Perugia and MUR for support within the project Vitality. DVU, MIS, GPG, KML, and AZV thank Ministry of Science and Higher Education for support of their work (project #121021000105-7) and Lomonosov Moscow State University Program of Development for opportunity to use NMR, X-ray, and chromatographic equipment. DVU and GPG also thank Konstantin A. Lyssenko for help with the X-ray measurements and refinements.

References

1 C. Ehm, J. Krüger and D. Lentz, How a Thermally Unstable Metal Hydrido Complex Can Yield High Catalytic Activity Even at Elevated Temperatures, *Chem. – Eur. J.*, 2016, **22**, 9305–9310.
2 T. Louis-Goff, H. V. Trinh, E. Chen, A. L. Rheingold, C. Ehm and J. Hyvl, Stabilizing Effect of Pre-equilibria: A Trifluoromethyl Complex as a CF2 Reservoir in Catalytic Olefin Difluorocarbenation, *ACS Catal.*, 2022, **12**, 3719–3730.
3 D. Y. Curtin and M. C. Crew, Rearrangement with Nitrous Acid of the Diastereoisomeric 1-p-Anisyl-1-phenyl-2-aminopropanols. The cis Effect of Methyl and Phenyl Groups1, *J. Am. Chem. Soc.*, 1955, **77**, 354–357.
4 V. Busico, R. Cipullo, R. Pellecchia, G. Talarico and A. Razavi, Hafnocenes and MAO: Beware of Trimethylaluminum!, *Macromolecules*, 2009, **42**, 1789–1791.
5 G. Ciancaleoni, N. Fraldi, P. H. M. Budzelaar, V. Busico and A. Macchioni, Structure and Dynamics in Solution of Bis

(phenoxy-amine)Zirconium Catalysts for Olefin Polymerization, *Organometallics*, 2011, **30**, 3096–3105.

6 G. Ciancaleoni, N. Fraldi, R. Cipullo, V. Busico, A. Macchioni and P. H. M. Budzelaar, Structure/Properties Relationship for Bis(phenoxyamine)Zr(IV)-Based Olefin Polymerization Catalysts: A Simple DFT Model To Predict Catalytic Activity, *Macromolecules*, 2012, **45**, 4046–4053.

7 L. Rocchigiani, V. Busico, A. Pastore and A. Macchioni, Probing the interactions between all components of the catalytic pool for homogeneous olefin polymerisation by diffusion NMR spectroscopy, *Dalton Trans.*, 2013, **42**, 9104–9111.

8 V. Busico, R. Cipullo, F. Cutillo, N. Friederichs, S. Ronca and B. Wang, Improving the Performance of Methylalumoxane: A Facile and Efficient Method to Trap "Free" Trimethylaluminum, *J. Am. Chem. Soc.*, 2003, **125**, 12402–12403.

9 L. Rocchigiani, V. Busico, A. Pastore, G. Talarico and A. Macchioni, Unusual Hafnium–Pyridylamido/ERn Heterobimetallic Adducts (ERn=ZnR2 or AlR3), *Angew. Chem., Int. Ed.*, 2014, **53**, 2157–2161.

10 C. Ehm, R. Cipullo, P. H. M. Budzelaar and V. Busico, Role (s) of TMA in polymerization, *Dalton Trans.*, 2016, **45**, 6847–6855.

11 M. Bochmann, The Chemistry of Catalyst Activation: The Case of Group 4 Polymerization Catalysts, *Organometallics*, 2010, **29**, 4711–4740.

12 F. Ghiotto, C. Pateraki, J. R. Severn, N. Friederichs and M. Bochmann, Rapid evaluation of catalysts and MAO activators by kinetics: what controls polymer molecular weight and activity in metallocene/MAO catalysts?, *Dalton Trans.*, 2013, **42**, 9040–9048.

13 K. P. Bryliakov, E. P. Talsi, A. Z. Voskoboynikov, S. J. Lancaster and M. Bochmann, Formation and Structures of Hafnocene Complexes in MAO- and AlBui3/CPh3[B(C6F5)4]-Activated Systems, *Organometallics*, 2008, **27**, 6333–6342.

14 G. Ciancaleoni, N. Fraldi, P. H. M. Budzelaar, V. Busico and A. Macchioni, Activation of a bis(phenoxy-amine) pre-catalyst for olefin polymerisation: first evidence for an outer sphere ion pair with the methylborate counterion, *Dalton Trans.*, 2009, 8824–8827, DOI: **10.1039/B908805A**.

15 E. Y. Tshuva, I. Goldberg and M. Kol, Isospecific Living Polymerization of 1-Hexene by a Readily Available NonmetalloceneC2-Symmetrical Zirconium Catalyst, *J. Am. Chem. Soc.*, 2000, **122**, 10706–10707.

16 A. Cohen, J. Kopilov, M. Lamberti, V. Venditto and M. Kol, Same Ligand, Different Metals: Diiodo–Salan Complexes of the Group 4 Triad in Isospecific Polymerization of 1-Hexene and Propylene, *Macromolecules*, 2010, **43**, 1689–1691.

17 S. Segal, I. Goldberg and M. Kol, Zirconium and Titanium Diamine Bis(phenolate) Catalysts for α-Olefin Polymerization: From Atactic Oligo(1-hexene) to Ultrahigh-Molecular-Weight Isotactic Poly(1-hexene), *Organometallics*, 2005, **24**, 200–202.

18 A. Yeori, S. Groysman, I. Goldberg and M. Kol, Diastereoisomerically Selective Enantiomerically Pure Titanium Complexes of Salan Ligands: Synthesis, Structure, and Preliminary Activity Studies, *Inorg. Chem.*, 2005, **44**, 4466–4468.

19 V. Busico, R. Cipullo, R. Pellecchia, S. Ronca, G. Roviello and G. Talarico, Design of stereoselective Ziegler–Natta propene polymerization catalysts, *Proc. Natl. Acad. Sci. U. S. A.*, 2006, **103**, 15321–15326.

20 C. Zuccaccia, V. Busico, R. Cipullo, G. Talarico, R. D. J. Froese, P. C. Vosejpka, P. D. Hustad and A. Macchioni, On the First Insertion of α-Olefins in Hafnium Pyridyl-Amido Polymerization Catalysts, *Organometallics*, 2009, **28**, 5445–5458.

21 G. P. Goryunov, M. I. Sharikov, A. N. Iashin, J. A. M. Canich, S. J. Mattler, J. R. Hagadorn, D. V. Uborsky and A. Z. Voskoboynikov, Rigid Postmetallocene Catalysts for Propylene Polymerization: Ligand Design Prevents the Temperature-Dependent Loss of Stereo- and Regioselectivities, *ACS Catal.*, 2021, **11**, 8079–8086.

22 C. Ehm, A. Vittoria, G. P. Goryunov, V. V. Izmer, D. S. Kononovich, P. S. Kulyabin, R. Di Girolamo, P. H. M. Budzelaar, A. Z. Voskoboynikov, V. Busico, D. V. Uborsky and R. Cipullo, A Systematic Study of the Temperature-Induced Performance Decline of ansa-Metallocenes for iPP, *Macromolecules*, 2020, **53**, 9325–9336.

23 P. S. Kulyabin, G. P. Goryunov, M. I. Sharikov, V. V. Izmer, A. Vittoria, P. H. M. Budzelaar, V. Busico, A. Z. Voskoboynikov, C. Ehm, R. Cipullo and D. V. Uborsky, ansa-Zirconocene Catalysts for Isotactic-Selective Propene Polymerization at High Temperature: A Long Story Finds a Happy Ending, *J. Am. Chem. Soc.*, 2021, **143**, 7641–7647.

24 V. Busico, R. Cipullo, N. Friederichs, S. Ronca, G. Talarico, M. Togrou and B. Wang, Block Copolymers of Highly Isotactic Polypropylene via Controlled Ziegler–Natta Polymerization, *Macromolecules*, 2004, **37**, 8201–8203.

25 P. Pracht, F. Bohle and S. Grimme, Automated exploration of the low-energy chemical space with fast quantum chemical methods, *Phys. Chem. Chem. Phys.*, 2020, **22**, 7169–7192.

26 M. J. Frisch, G. W. Trucks, H. B. Schlegel, G. E. Scuseria, M. A. Robb, J. R. Cheeseman, G. Scalmani, V. Barone, G. A. Petersson, H. Nakatsuji, X. Li, M. Caricato, A. V. Marenich, J. Bloino, B. G. Janesko, R. Gomperts, B. Mennucci, H. P. Hratchian, J. V. Ortiz, A. F. Izmaylov, J. L. Sonnenberg, D. Williams-Young, F. Ding, F. Lipparini, F. Egidi, J. Goings, B. Peng, A. Petrone, T. Henderson, D. Ranasinghe, V. G. Zakrzewski, J. Gao, N. Rega, G. Zheng, W. Liang, M. Hada, M. Ehara, K. Toyota, R. Fukuda, J. Hasegawa, M. Ishida, T. Nakajima, Y. Honda, O. Kitao, H. Nakai, T. Vreven, K. Throssell, J. A. Montgomery, Jr., J. E. Peralta, F. Ogliaro, M. J. Bearpark, J. J. Heyd, E. N. Brothers, K. N. Kudin, V. N. Staroverov, T. A. Keith, R. Kobayashi, J. Normand, K. Raghavachari, A. P. Rendell, J. C. Burant, S. S. Iyengar, J. Tomasi, M. Cossi, J. M. Millam, M. Klene, C. Adamo, R. Cammi, J. W. Ochterski, R. L. Martin, K. Morokuma, O. Farkas,

J. B. Foresman and D. J. Fox, *Gaussian 16, revision A.03*, Gaussian, Inc., Wallingford, CT, 2016.

27 J. M. Tao, J. P. Perdew, V. N. Staroverov and G. E. Scuseria, Climbing the density functional ladder: Nonempirical meta-generalized gradient approximation designed for molecules and solids, *Phys. Rev. Lett.*, 2003, **91**, 146401.

28 B. P. Pritchard, D. Altarawy, B. Didier, T. D. Gibson and T. L. Windus, New Basis Set Exchange: An Open, Up-to-Date Resource for the Molecular Sciences Community, *J. Chem. Inf. Model.*, 2019, **59**, 4814–4820.

29 P. Schwerdtfeger, The Pseudopotential Approximation in Electronic Structure Theory, *ChemPhysChem*, 2011, **12**, 3143–3155.

30 J. Tomasi, B. Mennucci and R. Cammi, Quantum Mechanical Continuum Solvation Models, *Chem. Rev.*, 2005, **105**, 2999–3094.

31 K. A. Peterson, D. Figgen, M. Dolg and H. Stoll, Energy-consistent relativistic pseudopotentials and correlation consistent basis sets for the 4d elements Y–Pd, *J. Chem. Phys.*, 2007, **126**, 124101.

32 Y.-S. Huang, J.-Q. Liu, L.-J. Zhang and H.-L. Lu, Synthesis of 1-Indanones from Benzoic Acids, *Ind. Eng. Chem. Res.*, 2012, **51**, 1105–1109.

33 P. C. B. Page, H. Heaney, M. J. McGrath, E. P. Sampler and R. F. Wilkins, Retro-Mannich reactions of 3-alkyl-3,4-dihydro-2H-1,3-benz[e]oxazines and the synthesis of axially chiral resorcinarenes, *Tetrahedron Lett.*, 2003, **44**, 2965–2970.

34 R. W. Van De Water and T. R. R. Pettus, o-Quinone methides: intermediates underdeveloped and underutilized in organic synthesis, *Tetrahedron*, 2002, **58**, 5367–5405.

35 A. Yeori, I. Goldberg, M. Shuster and M. Kol, Diastereomerically-Specific Zirconium Complexes of Chiral Salan Ligands: Isospecific Polymerization of 1-Hexene and 4-Methyl-1-pentene and Cyclopolymerization of 1,5-Hexadiene, *J. Am. Chem. Soc.*, 2006, **128**, 13062–13063.

36 A. Yeori, I. Goldberg and M. Kol, Cyclopolymerization of 1,5-Hexadiene by Enantiomerically-Pure Zirconium Salan Complexes. Polymer Optical Activity Reveals α-Olefin Face Preference, *Macromolecules*, 2007, **40**, 8521–8523.

37 A. Dall'Anese, P. S. Kulyabin, D. V. Uborsky, A. Vittoria, C. Ehm, R. Cipullo, P. H. M. Budzelaar, A. Z. Voskoboynikov, V. Busico, L. Tensi, A. Macchioni and C. Zuccaccia, *Inorg. Chem.*, 2023, DOI: **10.1021/acs.inorgchem.3c02153**.

38 Z. Liu, E. Somsook, C. B. White, K. A. Rosaaen and C. R. Landis, Kinetics of Initiation, Propagation, and Termination for the [rac-(C2H4(1-indenyl)2)ZrMe][MeB(C6F5)3]-Catalyzed Polymerization of 1-Hexene, *J. Am. Chem. Soc.*, 2001, **123**, 11193–11207.

39 G. Antinucci, B. Dereli, A. Vittoria, P. H. M. Budzelaar, R. Cipullo, G. P. Goryunov, P. S. Kulyabin, D. V. Uborsky, L. Cavallo, C. Ehm, A. Z. Voskoboynikov and V. Busico, Selection of Low-Dimensional 3-D Geometric Descriptors for Accurate Enantioselectivity Prediction, *ACS Catal.*, 2022, **12**, 6934–6945.

40 F. Zaccaria, C. Zuccaccia, R. Cipullo, P. H. M. Budzelaar, A. Macchioni, V. Busico and C. Ehm, BHT-Modified MAO: Cage Size Estimation, Chemical Counting of Strongly Acidic Al Sites, and Activation of a Ti-Phosphinimide Precatalyst, *ACS Catal.*, 2019, **9**, 2996–3010.

41 F. Zaccaria, P. H. M. Budzelaar, R. Cipullo, C. Zuccaccia, A. Macchioni, V. Busico and C. Ehm, Reactivity Trends of Lewis Acidic Sites in Methylaluminoxane and Some of Its Modifications, *Inorg. Chem.*, 2020, **59**, 5751–5759.

42 F. Zaccaria, C. Zuccaccia, R. Cipullo, P. H. M. Budzelaar, A. Macchioni, V. Busico and C. Ehm, On the Nature of the Lewis Acidic Sites in "TMA-Free" Phenol-Modified Methylaluminoxane, *Eur. J. Inorg. Chem.*, 2020, **2020**, 1088–1095.

43 J.-N. Pédeutour, K. Radhakrishnan, H. Cramail and A. Deffieux, Use of "TMA-depleted" MAO for the activation of zirconocenes in olefin polymerization, *J. Mol. Catal. A: Chem.*, 2002, **185**, 119–125.

44 R. A. Stapleton, B. R. Galan, S. Collins, R. S. Simons, J. C. Garrison and W. J. Youngs, Bulky Aluminum Alkyl Scavengers in Olefin Polymerization with Group 4 Catalysts, *J. Am. Chem. Soc.*, 2003, **125**, 9246–9247.

45 V. Murphy, X. Bei, T. R. Boussie, O. Brümmer, G. M. Diamond, C. Goh, K. A. Hall, A. M. Lapointe, M. Leclerc, J. M. Longmire, J. A. W. Shoemaker, H. Turner and W. H. Weinberg, High-Throughput Approaches for the Discovery and Optimization of New Olefin Polymerization Catalysts, *Chem. Rec.*, 2002, **2**, 278–289.

46 T. R. Boussie, G. M. Diamond, C. Goh, K. A. Hall, A. M. LaPointe, M. Leclerc, C. Lund, V. Murphy, J. A. W. Shoemaker, U. Tracht, H. Turner, J. Zhang, T. Uno, R. K. Rosen and J. C. Stevens, A Fully Integrated High-Throughput Screening Methodology for the Discovery of New Polyolefin Catalysts: Discovery of a New Class of High Temperature Single-Site Group (IV) Copolymerization Catalysts, *J. Am. Chem. Soc.*, 2003, **125**, 4306–4317.

47 Y. L. Dar, High-Throughput Experimentation: A Powerful Enabling Technology for the Chemicals and Materials Industry, *Macromol. Rapid Commun.*, 2004, **25**, 34–47.

48 T. R. Boussie, G. M. Diamond, C. Goh, K. A. Hall, A. M. LaPointe, M. K. Leclerc, V. Murphy, J. A. W. Shoemaker, H. Turner, R. K. Rosen, J. C. Stevens, F. Alfano, V. Busico, R. Cipullo and G. Talarico, Nonconventional Catalysts for Isotactic Propene Polymerization in Solution Developed by Using High-Throughput-Screening Technologies, *Angew. Chem., Int. Ed.*, 2006, **45**, 3278–3283.

49 V. Busico, R. Pellecchia, F. Cutillo and R. Cipullo, High-Throughput Screening in Olefin-Polymerization Catalysis: From Serendipitous Discovery Towards Rational Understanding, *Macromol. Rapid Commun.*, 2009, **30**, 1697–1708.

50 C. Ehm, A. Mingione, A. Vittoria, F. Zaccaria, R. Cipullo and V. Busico, High-Throughput Experimentation in Olefin Polymerization Catalysis: Facing the Challenges of Miniaturization, *Ind. Eng. Chem. Res.*, 2020, **59**, 13940–13947.

